

1 **Running head:** ???

2 Cranial morphological disparity within the
3 adaptive radiation of tenrecs (Afrosoricida,
4 Tenrecidae) is no greater than expected by
5 chance

6 Sive Finlay^{1,2,*} and Natalie Cooper^{1,2}

7 ¹ School of Natural Sciences, Trinity College Dublin, Dublin 2, Ireland.

8 ² Trinity Centre for Biodiversity Research, Trinity College Dublin, Dublin 2, Ireland.

9 *sfinlay@tcd.ie; Zoology Building, Trinity College Dublin, Dublin 2, Ireland.

10 Fax: +353 1 6778094; Tel: +353 1 896 2571.

11 **Keywords:** disparity, morphology, geometric morphometrics, tenrecs,
12 golden moles, adaptive radiation

¹³ **Abstract**

14 Introduction

15 Adaptive radiations, "evolutionary divergence of members of a single
16 phylogenetic lineage into a variety of different adaptive forms" (Futuyma
17 1998, cited by Losos, 2010) have long-attracted the interests and attentions
18 of naturalists. Some of the most famous examples include cichlid fish and
19 Caribbean *Anolis* lizards (Gavrilets & Losos, 2009). These groups exhibit
20 great variety in both their phenotypic forms and the ecological niches
21 which they occupy.

22 Each of these groups are uncontroversially accepted as examples of
23 adaptive radiations. However, there has been considerable debate about
24 how adaptive radiations should be defined (REFS) and how to distinguish
25 an adaptively radiated group from just a clade of apparently diverse
26 species. This is an important distinction because we need a consistent
27 means of identifying an adaptive radiation before we can investigate and
28 understand the selective pressures which cause adaptive radiations to
29 develop in some groups and not others (REFS).

30 One suggestion which has been proposed is that an adaptively
31 radiated clade should show exceptional (i.e. greater than expected by
32 chance) morphological and ecological diversity (Losos & Mahler, 2010). In
33 this case, a group of species would be considered exceptionally diverse if
34 they have more phenotypic and ecological diversity than their closest
35 relatives and also if they exhibit greater diversity than expected by chance.
36 However, few putative examples of adaptive radiations have been
37 characterised in this way. Under this definition it is equally important to
38 demonstrate exceptional diversity in both phenotypic variety and the
39 range of ecological niches which the species occupy. However, for the

40 purposes of this paper we will focus on the first criteria; investigating the
41 evidence for morphological variety.

42 Phenotypic diversity is commonly measured as morphological
43 disparity; the diversity of organic form (Foote, 1997; Erwin, 2007)). There
44 is no single definition of disparity and it can be calculated in many ways
45 including measures of morphospace occupation (e.g. Goswami et al., 2011;
46 Brusatte et al., 2008) and rate-based approaches that assess the amount of
47 directed change away from an ancestor (O'Meara et al., 2006; Price et al.,
48 2013). Analyses of disparity apply these alternative approaches depending
49 on whether the study is interested in current patterns of morphological
50 diversity or the rate at which they accumulate through time.

51 Here we investigate current patterns of morphological disparity in
52 tenrecs (Afrosoricida, Tenrecidae) to determine whether they represent an
53 adaptive radiation sensu (Losos & Mahler, 2010). The tenrec family is
54 comprised of 34 species, 31 of which are endemic to Madagascar (Olson,
55 2013). From a single common ancestor (Asher & Hofreiter, 2006),
56 Malagasy tenrecs diversified into a wide variety of descendant species
57 which convergently resemble distantly related insectivore mammals such
58 as shrews (*Microgale* tenrecs), moles (*Oryzorictes* tenrecs) and hedgehogs
59 (*Echinops* and *Setifer* tenrecs) (Eisenberg & Gould, 1969).

60 Tenrecs are often cited as an example of an adaptively radiated family
61 which exhibits exceptional morphological diversity (Soarimalala &
62 Goodman, 2011; Olson & Goodman, 2003; Eisenberg & Gould, 1969).
63 However, this apparent exceptional diversity is based on subjective
64 comparisons to other groups and it has not been tested quantitatively. If
65 tenrecs are exceptionally morphologically diverse then, following (Losos

66 & Mahler, 2010), tenrecs should be more morphologically disparate than
67 expected by chance and they should exhibit significantly more phenotypic
68 diversity than their nearest relatives, the golden moles (Afrosoricida,
69 Chrysochloridae). Here we test these predictions using cranial
70 morphology as a proxy for phenotypic diversity.

71 Using the most complete morphological data set of tenrecs and golden
72 moles to date we apply geometric morphometric analyses (Rohlf &
73 Marcus, 1993; Zelditch et al., 2012) to quantify morphological disparity
74 among our species. Our results indicate that, on average, tenrecs are more
75 phenotypically diverse than their closest relatives but their morphological
76 diversity is no greater than that which is expected to evolve by chance.
77 Therefore, under strict definitions, the designation of tenrecs as an
78 exceptional adaptive radiation may need to be reconsidered.

79 These findings highlight the vital importance of testing our common,
80 but often erroneous, expectations about patterns of morphological
81 disparity in groups that exhibit apparent high levels of diversity.

82 **Materials and Methods**

83 **Data collection**

84 **Morphological data collection**

85 One of us (SF) photographed cranial specimens of tenrecs and golden
86 moles at the Natural History Museum London (NHML), the Smithsonian
87 Institute Natural History Museum (SI), the American Museum of Natural
88 History (AMNH), Harvard's Museum of Comparative Zoology (MCZ)

89 and the Field Museum of Natural History, Chicago (FMNH). We
90 photographed the specimens with a Canon EOS 650D camera fitted with
91 an EF 100mm f/2.8 Macro USM lens using a standardised procedure to
92 minimise potential error (see supplementary material for details).

93 We collected pictures of the skulls in dorsal, ventral and lateral views
94 (right side of the skull) and of the outer (buccal) side of the right
95 mandibles. A full list of museum accession numbers and access to the
96 images can be found in the supplementary material.

97 In total we collected pictures from 182 skulls in dorsal view (148
98 tenrecs and 34 golden moles) and 181 mandibles in lateral view (147
99 tenrecs and 34 golden moles), representing 31 species of tenrec (out of the
100 total 34 in the family) and 12 species of golden moles (out of a total of 21
101 in the family (Asher et al., 2010)). We used the taxonomy of Wilson and
102 Reeder (2005) supplemented with more recent sources (IUCN, 2012;
103 Olson, 2013) to identify our specimens.

104 We used a combination of both landmarks (type 2 and type 3,
105 (Zelditch et al., 2012)) and semilandmarks to characterise the shapes of
106 our specimens. Our landmarks (points) and semilandmarks (outline
107 curves) used to represent shape variation in the dorsal skulls and
108 mandibles are depicted in Figures 1 and 2 respectively. Corresponding
109 landmark definitions for each view are in tables 1 and 2. We also placed
110 landmarks and semilandmarks on photographs of ventral and lateral skull
111 views, details can be found in the supplementary material. We digitised
112 all landmarks and semilandmarks in tpsDIG, version 2.17 (Rohlf, 2013).

113 We re-sampled the outlines to the minimum number of evenly spaced
114 points required to represent each outline accurately (MacLeod, 2013,

115 details in supplementary material). We used TPSUtil (Rohlf, 2012) to
116 create sliders files (Zelditch et al., 2012) to define which points were
117 semilandmarks. We conducted all subsequent analyses in R version 3.0.2
118 (R Development Core Team, 2013) within the geomorph package (Adams
119 et al., 2013). We used the gpagen function to run a general Procrustes
120 alignment (REFS) of the landmark coordinates while sliding the
121 semilandmarks by minimising procrustes distance rather than bending
122 energy (REFS). We used these Procrustes-aligned coordinates of all species
123 (n=43) to calculate average shape values for each species which we then
124 used for a principal components (PC) analysis (REFS) with the
125 plotTangentSpace function (Adams et al., 2013).

126 **Phylogeny**

127 Instead of basing our analyses on individual trees and assuming that their
128 topologies were known without error (e.g. Ruta et al., 2013; Foth et al.,
129 2012; Brusatte et al., 2008; Harmon et al., 2003) we used a distribution of
130 101 pruned phylogenies derived from the randomly resolved mammalian
131 supertrees in (Kuhn et al., 2011).

132 Eight species (six *Microgale* tenrecs and two golden moles) in our
133 morphological data were not in the phylogenies. Phylogenetic
134 relationships among the *Microgale* have not been resolved more recently
135 than the (Kuhn et al., 2011) analysis, therefore we added the additional
136 *Microgale* species at random to the *Microgale* genus within each phylogeny
137 (Revell, 2012). We could not use the same approach to add the two
138 missing golden mole species because they were the only representatives of
139 their respective genera within our data. Therefore we randomly added

140 these species to the common ancestral node (using the findMRCA function
141 in phytools (Revell, 2012)) of all golden moles within each phylogeny.
142 Adding these extra species to the phylogenies created polytomies which
143 we resolved arbitrarily using zero-length branches (Paradis et al., 2004).
144 We calculated pairwise phylogenetic distances among species using the
145 cophenetic function (R Development Core Team, 2013).

146 **Analyses**

147 **Disparity calculations**

148 We calculated morphological disparity separately for golden moles and
149 tenrecs in each of the morphological datasets. We used the PC axes which
150 accounted for 95% of the cumulative variation to calculate four disparity
151 metrics; the sum and product of the range and variance of morphospace
152 occupied by each family (Brusatte et al., 2008; Foth et al., 2012; Ruta et al.,
153 2013). We also calculated morphological disparity directly from the
154 Procrustes-superimposed shape data (ZelditchMD, Zelditch et al., 2012).
155 Disparity is expected to be higher in larger groups (REFS). Therefore we
156 repeated our disparity comparisons between the two families using
157 rarefaction (see supplementary material) to confirm that observed
158 differences in disparity between the two groups were not artefacts of
159 differences in sample size.

160 To test whether tenrecs are more morphologically disparate than
161 expected by chance, we simulated shape evolution (Harmon et al., 2008)
162 of the species-average, Procrustes-superimposed shape coordinates of
163 each tenrec species across our distribution of phylogenies. We took

164 "chance" to mean the expected shape evolution under a Brownian Motion
165 (BM) model and we repeated 1000 simulations on of shape evolution in
166 BM on each of 101 phylogenies pruned to include tenrec species only. We
167 ran a principal components analysis on each of the simulations and used
168 the PC axes which accounted for 95% of the cumulative variation to
169 calculate disparity metrics.

170 We compared the observed disparity measure to the corresponding
171 distribution of values and used a two-tailed test to determine whether the
172 observed (true) disparity measures were more or less than that which is
173 expected to evolve under BM.

174 The majority of tenrecs (19 out of 31 in our data) are members of the
175 *Microgale* (shrew-like) genus which is notable for its relatively low
176 phenotypic diversity (Soarimalala & Goodman, 2011; Jenkins, 2003) and
177 may mask signals of high disparity among other tenrecs. To test this we
178 repeated our simulations of shape evolution excluding *Microgale* species.
179 This reduced our data set for tenrecs from 31 to 12 species.

180 To test whether tenrecs have significantly different morphologies than
181 golden moles, we used a non parametric MANOVA (Anderson, 2001) to
182 compare morphospace occupation between the two groups (REFS?).

183 **Results**

184 **Morphological disparity in tenrecs**

185 We compared observed disparity to the distributions of expected disparity
186 calculated from BM simulations of shape data (1,000 simulations on each

187 of 101 phylogenies). We present the results from comparing our observed
188 and simulated measures of sum of variance (figures 3 and 4) because all
189 disparity metrics yielded the same patterns: tenrecs have significantly
190 lower disparity than expected under BM. Full results from all disparity
191 metrics and including the ventral and lateral skull views can be found in
192 the supplementary.

193 Removing the phenotypically similar *Microgale* tenrecs did not
194 qualitatively affect our results; the non-*Microgale* tenrecs still show
195 significantly lower phenotypic disparity than expected by chance
196 (simulation results in the supplementary material).

197 **Morphological disparity in tenrec and golden moles**

198 Figures 5 and 6 depict the morphospace plots derived from our principal
199 components analyses of average Procrustes-superimposed shape
200 coordinates for each species in our skull and mandible data respectively.
201 We used the principal components axes which accounted for 95% of the
202 cumulative variation ($n = 6$ axes for the dorsal skulls analysis and $n = 11$
203 axes for the mandibles) to calculate the disparity of each family.

204 In the dorsal skulls analysis, tenrecs and golden moles occupy
205 significantly different areas of morphospace (npMANOVA, $F = 59.34$, $R^2 =$
206 0.59 , $p = 0.001$) indicating that the two families have significantly different
207 skull morphologies. For each of the calculated metrics, tenrecs have
208 higher disparity than golden moles but these differences were not
209 significant for the variance-based calculations. Non-*Microgale* tenrecs also
210 higher disparity than golden moles but none of the comparisons were
211 statistically significant .

212 Tenrecs and golden moles have significantly different mandible shapes
213 (npMANOVA $F = 59.34$, $R^2 = 0.59$, $p = 0.001$). However, unexpectedly,
214 golden moles appear to have higher disparity than tenrecs in the shape of
215 their mandibles (although these differences are only significant when
216 disparity is calculated as product of variance or ZelditchMD).

217 We tested whether these results may be artefacts of relatively low
218 phenotypic diversity within *Microgale* tenrecs. However, although golden
219 moles and non-*Microgale* tenrecs occupy significantly different areas of
220 morphospace (npMANOVA $F = 31.6$, $R^2 = 0.59$, $p = 0.001$), there is no
221 significant difference between the two groups for any metrics of disparity.

222 Discussion

223 Our findings provide new insights into phenotypic diversity within the
224 tenrec family. Contrary to previous suggestions (e.g. Eisenberg & Gould,
225 1969; Olson, 2013), tenrecs do not appear to be exceptional in their
226 morphological diversity. Tenrecs are not more morphologically varied
227 than expected to evolve by chance: they show significantly lower disparity
228 in their morphologies than expected to evolve under Brownian Motion
229 models of evolution.

230 When we compared tenrecs' cranial morphologies to their closest
231 relatives the resulting patterns were less straightforward. For the analyses
232 of skull shapes we found a trend towards higher disparity in tenrecs than
233 in golden moles although these apparent differences were only significant
234 for some disparity metrics. In contrast, the analyses of the mandibles
235 indicated that golden moles have more diverse mandible shapes although,

236 again, these results are only significant for some disparity metrics.

237 These results put a new perspective on the long-standing assumption
238 that tenrecs are an adaptive radiation.

239 It is evidence that tenrecs are a diverse group, both phenotypically and
240 ecologically. Body sizes of extant tenrecs span three orders of magnitude
241 (2.5 to >2,000g) which is a greater range than all other Families, and most
242 Orders, of living mammals (Olson & Goodman, 2003). Within this vast
243 size range there is striking morphological diversity, from the spiny
244 *Echinops*, *Setifer* and striking *Hemicentetes* to the shrew-like *Microgale*.
245 Furthermore, tenrecs inhabit a variety of ecological niches and habitats
246 including terrestrial, arboreal, semi-aquatic and semi-fossorial forms
247 (REFS). However, our results cast doubt over whether the evident
248 diversity within the tenrec family should be considered to be a true
249 adaptive radiation.

250 Phenotypic and ecological divergences within a clade are not
251 surprising; most clades have at least small levels of disparity so, when it
252 comes to identifying adaptive radiations, it's important to identify clades
253 which are exceptional in their diversity (Losos & Mahler, 2010). Here we
254 have presented the first quantitative investigation of morphological
255 disparity in tenrecs and our results suggest that perhaps phenotypic
256 variation in tenrecs is not the product of an adaptive radiation in the strict
257 sense of its definition.

258 All of our simulation analyses agree that tenrecs show significantly
259 lower morphological diversity than that which is expected to evolve under
260 random, BM evolution.

261 The discrepancies between our analyses of cranial and mandible

262 disparity could reflect derive from factors associated with the modularity
263 of morphological evolution.

264 There is strong evidence that morphological variation in skulls and
265 mandibles is derived from differential evolution of integrated
266 developmental modules (reviewed by Klingenberg, 2013). For example,
267 there seems to be two primary modules in the mouse mandible; an
268 alveolar part which holds the teeth and the ascending ramus for muscle
269 attachment and which articulates with the skull (Klingenberg, 2008).
270 Geometric shape covariation is stronger within rather than between these
271 modules.

272 Our landmarks and curves for the mandibles (figure 2, table 2) include
273 aspects of variation in the dentition but they focus particular attention on
274 the ascending ramus (condyloid, condylar and angular processes).
275 Therefore the higher morphological disparity in golden mole mandibles
276 most likely reflects greater variation in the shape of the muscle attachment
277 areas of the mandible. In contrast it proved impossible to position reliable
278 landmarks on the corresponding articulation areas of the skull in lateral
279 view (see supplementary).

280 If variation in muscle attachment/articulation sites is driving
281 morphological disparity in mandibles, it is not clear why golden moles
282 should have more disparate articular rami than tenrecs.

283 While our findings cast doubt on the designation of tenrecs as an
284 adaptive radiation *sensu* (Losos & Mahler, 2010), there are certain caveats
285 to consider which could modify the interpretation of our results.

286 Phenotypic variation can evolve for reasons other than adaptive
287 radiation. Therefore, to describe phenotypic divergence as the product of

288 an adaptive radiations requires exceptional morphological diversity in
289 traits which have specific and proven adaptive significance (Losos &
290 Mahler, 2010). The evolution of cranial shape (both upper skull and
291 mandible), particularly dental morphology, has obvious correlations with
292 dietary specialisations (REFS) and occupation of specific ecological niches
293 (REFS).

294 Considering the wide ecological diversity of our study species; the
295 fossorial golden moles and semi-fossorial, arboreal, terrestrial and
296 semi-aquatic tenrecs (REFS) it is reasonable to expect that variation in
297 cranial shape should be an adaptive characteristic which allows the
298 animals to survive in their divergent niches. Therefore quantifying the
299 diversity of cranial morphology is a reasonable method of assessing the
300 significance of morphological variety within the context of identifying an
301 adaptive radiation.

302 Cranial shape similarities are commonly used to delineate species
303 boundaries (REFS) or for cross-taxonomic comparative studies of
304 phenotypic (dis)similarities (REFS). However, disparity studies are
305 inevitably constrained to be measures of diversity within specific traits
306 rather than overall morphology (Roy & Foote, 1997). Therefore it is
307 possible that other morphological proxies of phenotype; analyses of linear
308 measurements and/or discrete characters of either cranial or post-cranial
309 morphologies could yield different results.

310 However, the results of (Foth et al., 2012) are encouraging. In an
311 analysis of morphological disparity in pterosaurs, they found that
312 disparity calculations based on geometric morphometric characterisation
313 of skull shape yielded broadly similar results compared to analyses of

314 whole-skeleton discrete characters and limb proportion data sets.
315 Therefore the disparity patterns we find here based on geometric
316 morphometric analyses of cranial shape most likely represent
317 approximations of disparity which are accurate for morphological
318 diversity in the clades.

319 **Acknowledgements**

320 We thank Dr. François Gould, Thomas Guillerme and the members of
321 NERD club for insightful discussions and the museum staff and curators
322 for their support and access to collections. Funding was provided by an
323 Irish Research Council EMBARK Initiative Postgraduate Scholarship (SF)
324 and the European Commission CORDIS Seventh Framework Programme
325 (FP7) Marie Curie CIG grant. Proposal number: 321696 (NC, SF)

326 **References**

- 327 Adams, D., Otárola-Castillo, E. & Paradis, E. 2013. geomorph: an r
328 package for the collection and analysis of geometric morphometric
329 shape data. *Methods in Ecology and Evolution* **4**: 393–399.
330 10.1111/2041-210X.12035.
- 331 Anderson, M. 2001. A new method for non-parametric multivariate
332 analysis of variance. *Austral Ecology* **26**: 32–46.
333 10.1111/j.1442-9993.2001.01070.pp.x.
- 334 Asher, R. & Hofreiter, M. 2006. Tenrec phylogeny and the noninvasive
335 extraction of nuclear DNA. *Systematic Biology* **55**: 181–194.

- 336 Asher, R.J., Maree, S., Bronner, G., Bennett, N., Bloomer, P., Czechowski,
337 P., Meyer, M. & Hofreiter, M. 2010. A phylogenetic estimate for golden
338 moles (Mammalia, Afrotheria, Chrysochloridae). *BMC Evolutionary*
339 *Biology* **10**: 1–13.
- 340 Brusatte, S., Benton, M., Ruta, M. & Lloyd, G. 2008. Superiority,
341 competition and opportunism in the evolutionary radiation of
342 dinosaurs. *Science* **321**: 1485–1488.
- 343 Eisenberg, J.F. & Gould, E. 1969. The Tenrecs: A Study in Mammalian
344 Behaviour and Evolution. *Smithsonian Contributions to Zoology* **27**: 1–152.
- 345 Erwin, D. 2007. Disparity: morphological pattern and developmental
346 context. *Palaeontology* **50**: 57–73.
- 347 Foote, M. 1997. The evolution of morphological diversity. *Annual Review of*
348 *Ecology and Systematics* **28**: 129–152.
- 349 Foth, C., Brusatte, S. & Butler, R. 2012. Do different disparity proxies
350 converge on a common signal? Insights from the cranial morphometrics
351 and evolutionary history of *Pterosauria* (Diapsida: Archosauria). *Journal*
352 *of Evolutionary Biology* **25**: 904–915. 10.1111/j.1420-9101.2012.02479.x.
- 353 Gavrilets, S. & Losos, J. 2009. Adaptive radiation: contrasting theory with
354 data. *Science* **323**: 732–736. 10.1126/science.1157966.
- 355 Goswami, A., Milne, N. & Wroe, S. 2011. Biting through constraints:
356 cranial morphology, disparity and convergence across living and fossil
357 carnivorous mammals. *Proceedings of the Royal Society B: Biological*
358 *Sciences* **278**: 1831–1839. 10.1098/rspb.2010.2031.

- 359 Harmon, L., Schulte, J., Larson, A. & Losos, J.B. 2003. Tempo and mode of
360 evolutionary radiation in iguanian lizards. *Science* **301**: 961–964.
- 361 Harmon, L., Weir, J., Brock, C., Glor, R. & Challenger, W. 2008. GEIGER:
362 investigating evolutionary radiations. *Bioinformatics* **24**: 129–131.
- 363 Hopkins, M. 2013. Decoupling of taxonomic diversity and morphological
364 disparity during decline of the Cambrian trilobite family *Pterocephaliidae*.
365 *Journal of Evolutionary Biology* **26**: 1665–1676. 10.1111/jeb.12164.
- 366 IUCN 2012. International Union for Conservation of Nature.
- 367 Jenkins, P. 2003. *Microgale, shrew tenrecs*, pp. 1273–1278. The University of
368 Chicago Press, Chicago.
- 369 Klingenberg, C. 2008. Morphological integration and developmental
370 modularity. *Annual review of ecology, evolution, and systematics* **39**:
371 115–132.
- 372 Klingenberg, C. 2013. Cranial integration and modularity: insights into
373 evolution and development from morphometric data. *Hystrix, the Italian*
374 *Journal of Mammalogy* **24**: 43–58.
- 375 Kuhn, T., Mooers, A. & Thomas, G. 2011. A simple polytomy resolver for
376 dated phylogenies. *Methods in Ecology and Evolution* **2**: 427–436.
377 10.1111/j.2041-210X.2011.00103.x.
- 378 Losos, J. 2010. Adaptive radiation, ecological opportunity, and
379 evolutionary determinism. American Society of Naturalists E. O. Wilson
380 Award Address. *The American Naturalist* **175**: 623–639. 10.1086/652433.

- 381 Losos, J.B. & Mahler, D. 2010. *Adaptive radiation: the interaction of ecological*
382 *opportunity, adaptation and speciation*, chap. 15, pp. 381–420. Sinauer
383 Association, Sunderland, MA.
- 384 MacLeod, N. 2013. Landmarks and semilandmarks: Difference without
385 meaning and meaning without difference.
- 386 Olson, L. & Goodman, S. 2003. *Phylogeny and biogeography of tenrecs*, pp.
387 1235–1242. The University of Chicago Press, Chicago.
- 388 Olson, L.E. 2013. Tenrecs. *Current Biology* **23**: R5–R8.
- 389 O’Meara, B., Ané, C., Sanderson, M. & Wainwright, P. 2006. Testing for
390 different rates of continuous trait evolution using likelihood. *Evolution*
391 **60**: 922–933. 10.1111/j.0014-3820.2006.tb01171.x.
- 392 Paradis, E., Claude, J. & Strimmer, K. 2004. Ape: Analyses of
393 Phylogenetics and Evolution in R language. *Bioinformatics* **20**: 289–290.
394 10.1093/bioinformatics/btg412.
- 395 Price, S., Tavera, J., Near, T. & Wainwright, P. 2013. Elevated rates of
396 morphological and functional diversification in reef-dwelling haemulid
397 fishes. *Evolution* **67**: 417–428. 10.1111/j.1558-5646.2012.01773.x.
- 398 Revell, L. 2012. phytools: an R package for phylogenetic comparative
399 biology (and other things). *Methods in Ecology and Evolution* **3**: 217–223.
- 400 Rohlf, F. 2012. Tpsutil.
- 401 Rohlf, F. 2013. Tpsdig2 ver 2.17.
- 402 Rohlf, J. & Marcus, L. 1993. A revolution in morphometrics. *Trends in*
403 *Ecology & Evolution* **8**: 129–132.

- 404 Roy, K. & Foote, M. 1997. Morphological approaches to measuring
405 biodiversity. *Trends in Ecology & Evolution* **12**: 277–281.
- 406 Ruta, M., Angielczyk, K., Fröbisch, J. & Benton, M. 2013. Decoupling of
407 morphological disparity and taxic diversity during the adaptive
408 radiation of anomodont therapsids. *Proceedings of the Royal Society B:*
409 *Biological Sciences* **280**: 20131071. 10.1098/rspb.2013.1071.
- 410 Soarimalala, V. & Goodman, S. 2011. *Les petits mammifères de Madagascar*.
411 Guides sur la diversité biologique de Madagascar. Association Vahatra,
412 Antananarivo, Madagascar.
- 413 Team, R.D.C. 2013. R: A language and environment for statistical
414 computing.
- 415 Wilson, D. & Reeder, D. 2005. *Mammal species of the world. A taxonomic and*
416 *geographic reference (3rd ed)*. Johns Hopkins University Press.
- 417 Zelditch, M., Swiderski, D. & Sheets, D. 2012. *Geometric Morphometrics for*
418 *Biologists, second edition*. Academic Press, Elsevier, United States of
419 America.

List of Figures

421	1	Landmarks (red points) and curves (blue lines) used to capture the morphological shape of skulls in dorsal view. Curves were re-sampled to the same number of evenly-spaced points. See table X for description of curves and landmarks.	
422		<i>Potamogale</i>	
423		<i>velox</i> (Tenrecidae) skull, accession number: AMNH_51327 . . .	21
424			
425	2	Landmarks (red points) and curves (blue lines) used to capture the morphological shape of mandibles. Curves were re-sampled to the same number of evenly-spaced points. See table X for description of curves and landmarks.	
426		<i>Potamogale</i>	
427		<i>velox</i> (Tenrecidae) mandible, accession number: AMNH_51327	22
428			
429	3	Comparison of the observed and expected disparity in the dorsal skulls. Disparity is measured as sum of variance, blue arrow points to the observed value of disparity (0.0017) . . .	23
430			
431	4	Comparison of the observed and expected disparity in the mandibles. Disparity is measured as sum of variance, blue arrow points to the observed value of disparity (0.0031) . . .	24
432			
433	5	Principal components plot of the dorsal skulls' morphospace occupied by tenrecs (red, n=31) and golden moles (black, n=12). Axes are PC1 and PC2 of the average scores from a PCA analysis of mean Procrustes shape coordinates for each species.	25
434			
435	6	Principal components plot of the mandibles' morphospace occupied by tenrecs (red, n=31) and golden moles (black, n=12). Axes are PC1 and PC2 of the average scores from a PCA analysis of mean Procrustes shape coordinates for each species.	
436			
437			
438			
439			
440			
441			
442			
443			
444			
445			
446			

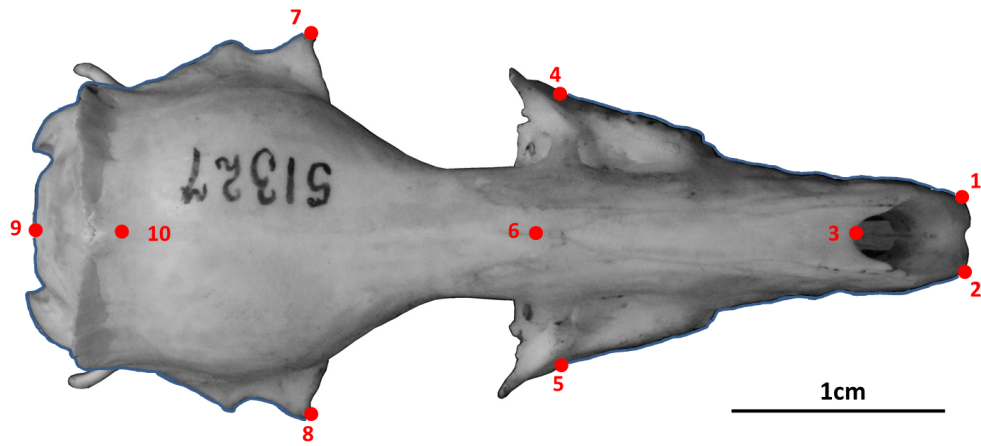


Figure 1: Landmarks (red points) and curves (blue lines) used to capture the morphological shape of skulls in dorsal view. Curves were re-sampled to the same number of evenly-spaced points. See table X for description of curves and landmarks. *Potamogale velox* (Tenrecidae) skull, accession number: AMNH_51327

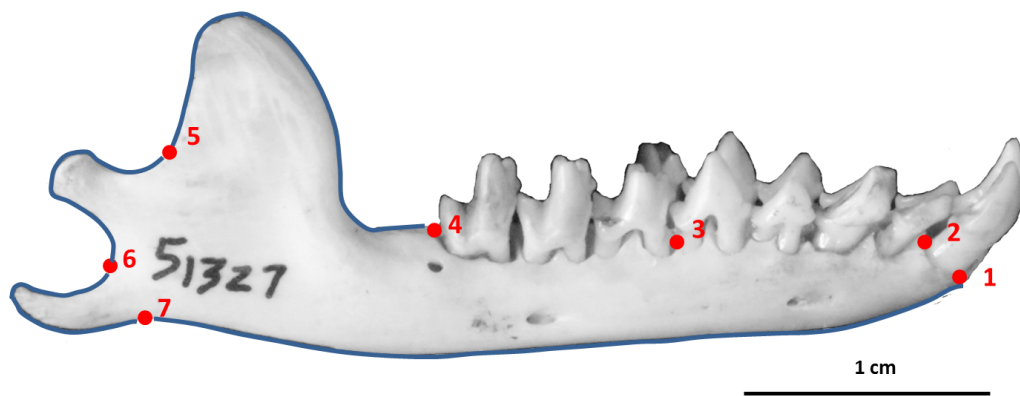


Figure 2: Landmarks (red points) and curves (blue lines) used to capture the morphological shape of mandibles. Curves were re-sampled to the same number of evenly-spaced points. See table X for description of curves and landmarks. *Potamogale velox* (Tenrecidae) mandible, accession number: AMNH_51327

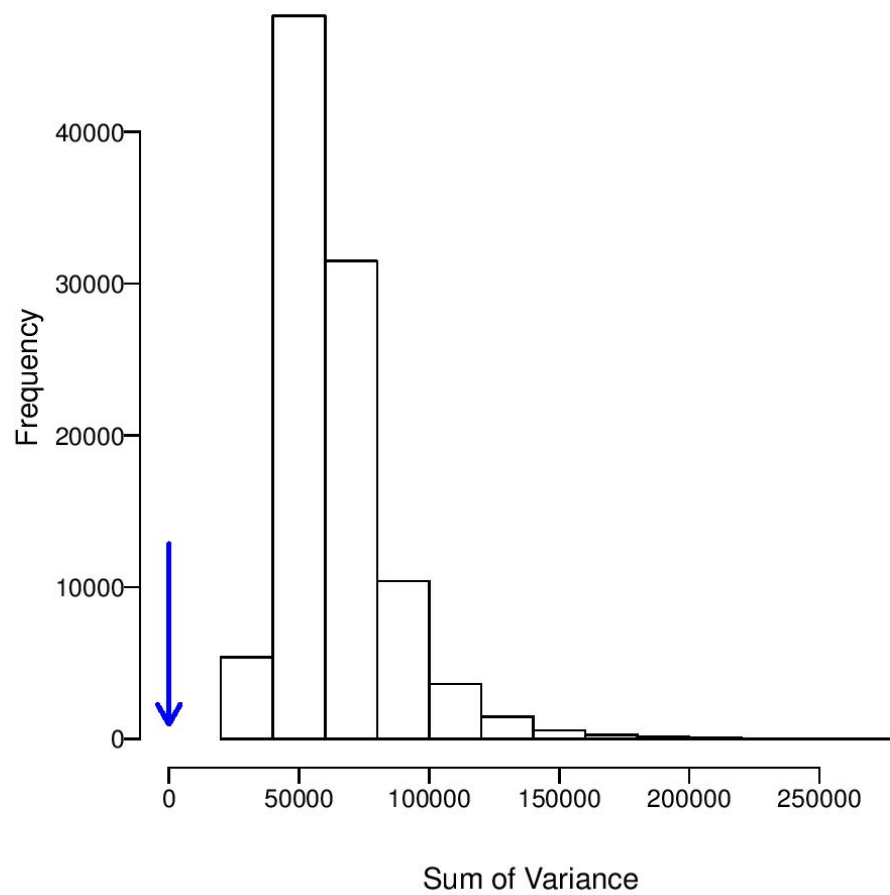


Figure 3: Comparison of the observed and expected disparity in the dorsal skulls. Disparity is measured as sum of variance, blue arrow points to the observed value of disparity (0.0017)

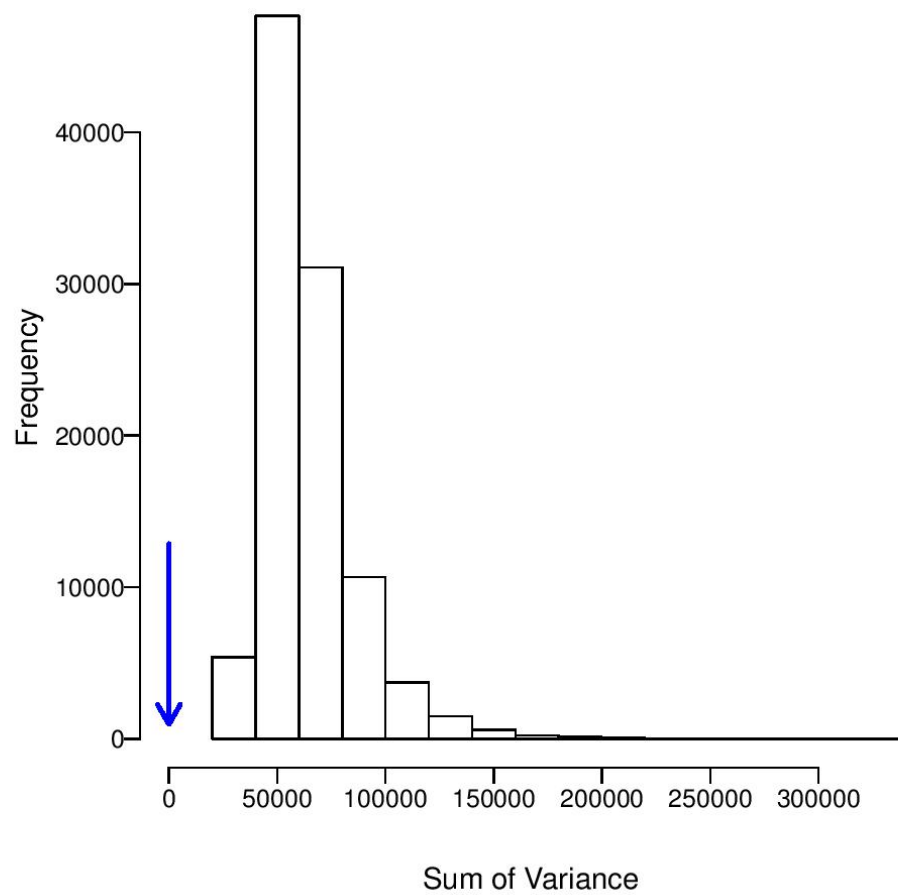


Figure 4: Comparison of the observed and expected disparity in the mandibles. Disparity is measured as sum of variance, blue arrow points to the observed value of disparity (0.0031)

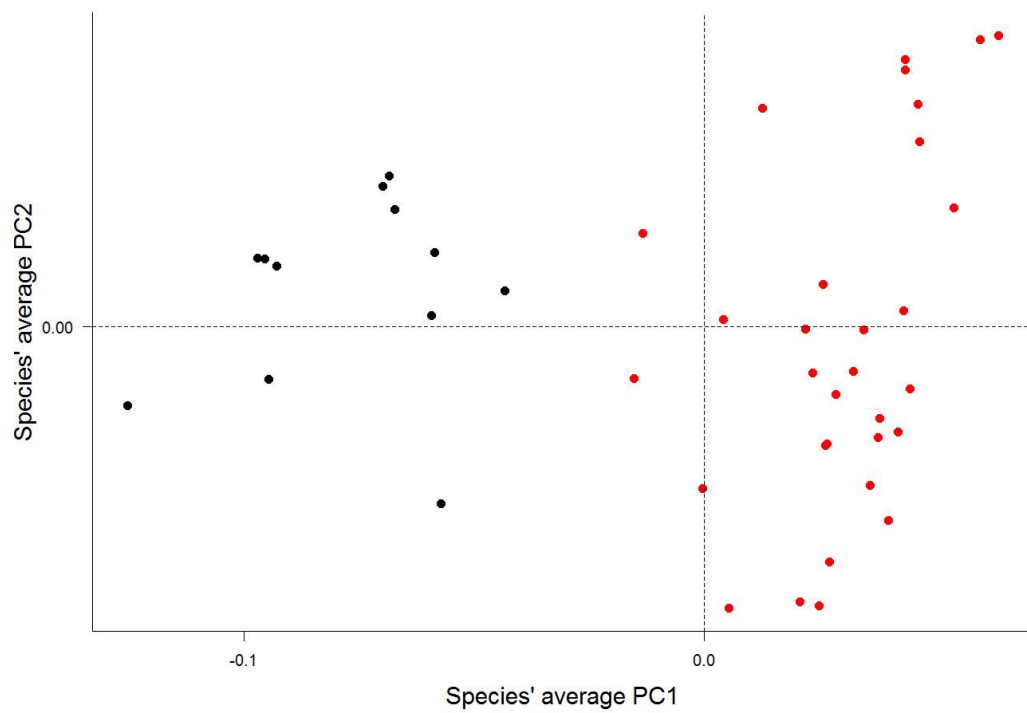


Figure 5: Principal components plot of the dorsal skulls' morphospace occupied by tenrecs (red, $n=31$) and golden moles (black, $n=12$). Axes are PC1 and PC2 of the average scores from a PCA analysis of mean Procrustes shape coordinates for each species.

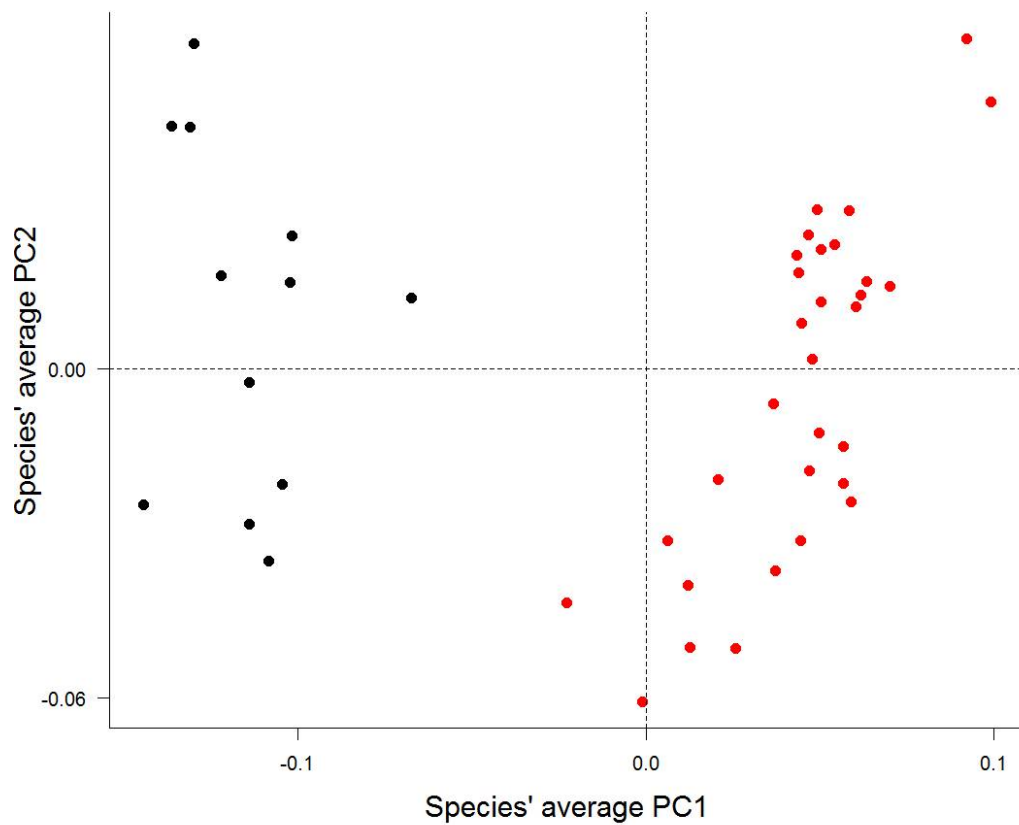


Figure 6: Principal components plot of the mandibles' morphospace occupied by tenrecs (red, $n=31$) and golden moles (black, $n=12$). Axes are PC1 and PC2 of the average scores from a PCA analysis of mean Procrustes shape coordinates for each species.

447 **List of Tables**

448	1	Descriptions of the landmarks (points) and curves (semi-	
449		landmarks) for the skulls in dorsal view (see Figure 1).	28
450	2	Descriptions of the landmarks (points) and curves (semi-	
451		landmarks) for the mandibles in lateral (buccal) view (see	
452		figure 2)	29

Table 1: Descriptions of the landmarks (points) and curves (semilandmarks) for the skulls in dorsal view (see Figure 1).

Landmark	Description
1 + 2	Left (1) and right (2) anterior points of the premaxilla
3	Anterior of the nasal bones in the midline
4 + 5	Maximum width of the palate (maxillary) on the left (4) and right (5)
6	Midline intersection between nasal and frontal bones
7 + 8	Widest point of the skull on the left (7) and right (8)
9	Posterior of the skull in the midline
10	Posterior intersection between saggital and parietal sutures
Curve A (12 points)	Outline of the braincase on the left side, between landmarks 9 and 7 (does not include visible features from the lower (ventral) side of the skull)
Curve B (10 points)	Outline of the palate on the left side, between landamarks 4 and 1 (outline of the rostrum only, not the shape of the teeth)
Curve C (12 points)	Outline of the braincase on the right side, between landmarks 9 and 8 (does not include visible features from the lower (ventral) side of the skull)
Curve D (10 points)	Outline of the palate on the right side, between landamarks 5 and 2 (outline of the rostrum only, not the shape of the teeth)

Table 2: Descriptions of the landmarks (points) and curves (semilandmarks) for the mandibles in lateral (buccal) view (see figure 2)

Landmark	Description
1	Anterior of the alveolus of the first incisor
2	Posterior of the alveolus of the first incisor
3	Anterior of the alveolus of the first molar
4	Posterior of the alveolus of the last molar
5	Maximum curvature between the coronoid and condylar processes
6	Maximum curvature between the condylar and angular processes
7	Maximum curvature between the angular process and the horizontal ramus
Curve A	Condylar process (between landmarks 4 and 5, 15 points)
Curve B	Condylar process (between landmarks 5 and 6, 15 points)
Curve C	Angular process (between landmarks 6 and 7, 15 points)
Curve D	Base of the jaw (between landmarks 7 and 1, 12 points)